

## Post seismic relaxation processes in the Aegean-Anatolian system: insights from space geodetic data (GPS) and geological/geophysical evidence

N. CENNI, F. D'ONZA, M. VITI, E. MANTOVANI, D. ALBARELLO and D. BABBUCCI

*Department of Earth Sciences, University of Siena, Italy*

(Received June 22, 2001; accepted October 10, 2001)

**Abstract** - Variation of motion rates and stress redistribution in the Anatolian-Aegean region induced by the last sequence of strong earthquakes occurring along the North Anatolian fault system since 1939 are investigated by a 2D numerical approach. The model is constituted by an elastic lithosphere coupled with a viscous asthenosphere. The predicted perturbations of the velocity field may account for the major features of the present day kinematic pattern in the study area, inferred from space geodetic data (GPS). This result can provide a possible explanation for the considerable difference between the long term average motion rates (5-10 mm /y), deduced by fault offset measurements along the North Anatolian fault and by the seismic history of this fault, and the geodetic velocities (20-30 mm /y) in the Anatolian-Aegean system. Furthermore, the slow migration of the velocity perturbations in the lithosphere, controlled by the coupling with the viscous asthenosphere, can explain the fact that the present day average velocity in the Aegean area (32 mm /y) is higher than those observed in western (24 mm /y) and eastern Anatolia (18 mm /y). The computed post seismic strain energy rate redistribution can also account for the time pattern of the seismicity rate in the study area during the last 60 years. The results obtained in this work might also have implications for the understanding of the geodynamic setting in the Mediterranean area, in that they indicate that the higher motion rates observed in the Aegean region with respect to those in Anatolia must not necessarily be interpreted as an effect of a slab pull mechanism in the Hellenic trench.

---

Corresponding author: E. Mantovani, Department of Earth Sciences, University of Siena, Via Laterina 8, Siena, Italy; phone: +39 0577233819/22; fax +39 0577233820; e-mail: mantovani@unisi.it

## 1. Introduction

It is recognized that strong earthquakes occurring in a rheological Earth can trigger a redistribution of displacements, strains and stresses (e.g. Elsasser, 1969; Anderson, 1975; Rydelek and Sacks, 1990). These perturbations propagate at rates much slower than those of seismic waves, due to the coupling of the lithosphere with the underlying viscous asthenosphere. Quantifications of this phenomenon by simplified diffusion models have provided possible explanations for the space-time distribution of major earthquakes in circumpacific zones (e.g. Anderson, 1975; Pollitz et al., 1998) and in the Anatolian-Aegean area (Mantovani et al., 2001a). The ever growing amount of space geodetic data provides a very powerful tool to improve our knowledge on post-seismic relaxation processes. In this work, attention is focused on the Anatolian-Aegean region, where a dense network of GPS mobile stations has allowed the development of a fairly accurate reconstruction of the present day kinematic pattern (e.g. McClusky et al., 2000). This evidence identifies three domains where the distribution of velocities with respect to stable Eurasia appears to be fairly uniform: eastern Anatolia, with an average rate of 18 mm /y, western Anatolia, with an average rate of 24 mm /y, and the Aegean, with an average rate of 32 mm /y (Fig. 1).

Some major features of this pattern cannot simply be reconciled with the long term kinematic behavior of the Anatolian-Aegean system deduced by geological and geophysical evidence. First of all, geodetic velocities, 18-32 mm /y, are significantly higher than the average rates, lower than 10 mm /y, inferred from geological and seismological information. Geological estimates are based on measurements of fault offsets developed along various segments of the North Anatolian fault (NAF) since the early Pliocene. These observations indicate a fairly regular distribution of values from roughly 40 km, at the NAF's easternmost edge, to roughly 25 km, at the Marmara zone (see Barka, 1992 and references therein). In terms of slip rate, the

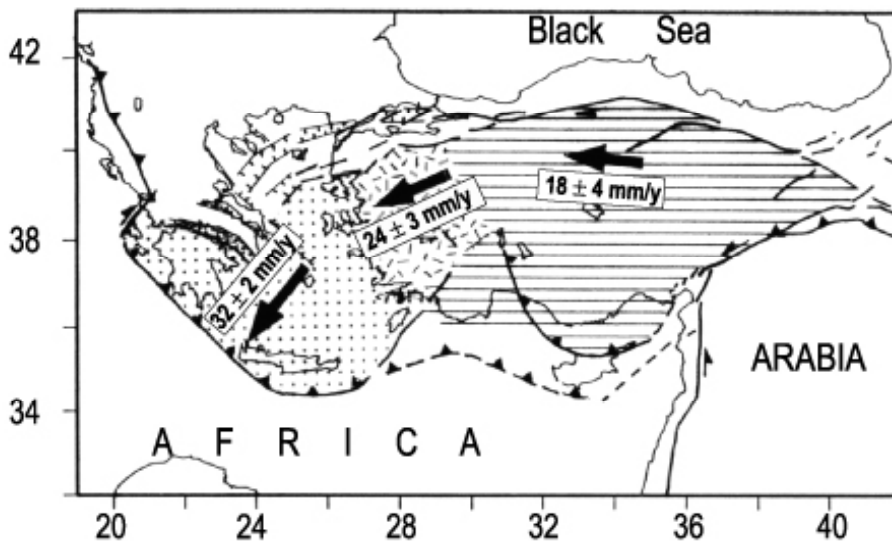


**Fig. 1** - Average geodetic (GPS) velocities (McClusky et al., 2000) in three central - eastern Mediterranean zones, Aegea (dotted), western (stepped) and eastern (dashed) Anatolia, which show a rather uniform kinematic behavior.

above evidence implies values ranging between 10 and 5 mm /y (Barka, 1992). Comparable values of slip rates (6-16 mm /y) have been obtained by trench studies along some segments of the NAF (Ikeda, 1988; Ikeda et al., 1991).

Other estimates of slip rates along the NAF can also be obtained by the analysis of the seismic history of this fault. Historical records indicate that major earthquake sequences, like the one that started in 1939, may have return periods of roughly 900 years (Ambraseys, 1988). Considering that during the last sequence seismic slips up to 7 meters have occurred (Barka, 1992), one can estimate that during one cycle the average rate is roughly 8 mm/y, in good agreement with geological estimates.

The average slip rate along the NAF could also be estimated by summing the moment tensors of earthquakes (Kostrov, 1974). Current values of strain rate obtained by applying this approach to the seismic history of the last 90 years, range from 27 to 40 mm /y (Jackson and McKenzie, 1984, 1988; Pondrelli et al., 1995). However, the reliability of this kind of estimate is very poorly defined (Viti et al., 2001). It might be strongly affected, e.g., by the inaccuracy of the scalar moment-magnitude relationship. The effect of this source of uncertainty is pointed out by the large interval of possible values of velocity (25-80 mm /yr) obtained by Jackson and McKenzie (1988). Furthermore, this kind of estimate might be considerably different from the long term deformation rate, due to the short time interval covered by available data with respect to the estimated long term pattern of seismic activity (Ambraseys, 1988). In particular, one must be aware that, in the period considered for computations, seismic activity could have been higher than normal since the data set includes one of the major seismic sequences which rarely affect this zone (Ambraseys, 1988).

Another major feature of the geodetic kinematic pattern (Fig. 1) is the fact that the Aegean velocities (32 mm /y) are higher than those of Anatolia (18-24 mm /y). This evidence might have important implications on the geodynamic setting of this zone. In particular, it might favour the hypothesis that the Aegean deformation pattern is mainly driven by a trench suction force in the Hellenic consuming boundary, induced by the gravitational sinking of the Ionian subducted lithosphere (e.g. Le Pichon et al., 1995; Meijer and Wortel, 1996; McClusky et al., 2000), with respect to the hypothesis that the main driving force is constituted by the E-W convergence between the Anatolian and Adriatic blocks (e.g. Tapponnier, 1977; Taymaz et al., 1991; Mantovani et al., 1997, 2000a, b). However, as argued by Mantovani et al. (2000a, 2000b), the implications of the first interpretation cannot easily be reconciled with major features of the present day strain field and of the Pliocenic time-space distribution of deformation in the Aegean and surrounding regions. Furthermore, numerical modeling experiments have shown that the complex pattern of strain styles in the central-eastern Mediterranean area can be satisfactorily reproduced by adopting the convergence of the confining plates (Africa - Arabia, Eurasia) as the unique driving mechanism (Mantovani et al., 2000b, 2001b).

A third interesting feature of the geodetic kinematic pattern is the mostly uniform distribution of velocities within the Aegean domain (McClusky et al., 2000), which would indicate that this area moves as an almost rigid block. However, these kinematics could not account for the recent strain field in the Aegean area, deduced by neotectonic data (e.g. Mercier

et al., 1989), since a uniform motion of the whole Aegean area would not be compatible with the widely recognized tensional tectonic activity in the southern (Cretan sea) and northern (northern trough) parts of the Aegean Sea.

The above evidence and arguments suggest that the kinematics of the Aegean-Anatolian system depicted by geodetic data is significantly different from the middle-long term kinematic behavior of these zones inferred from geological evidence and seismicity data. To find a possible explanation for this difference one could explore the possibility that the present day kinematic pattern of the study area is still under the influence of post-seismic relaxation processes induced by the last major westward jump of Anatolia, triggered by the strong 1939 Erzincan earthquake (Fig. 2; Barka, 1992). The hypothesis that plate motions are not uniform over time, being characterized by successive accelerations, is supported by significant evidence in circumpacific zones and by quantifications of post - seismic relaxation processes in rheological models (e.g. Anderson, 1975). The seismic history of the NAF (e.g. Ambraseys, 1988) suggests that the above concepts might also be applied to the Anatolian block. In this case, a big jump of the Anatolian extruding wedge seems to occur roughly every 900 years (Ambraseys, 1988). As discussed above, the average drifting rate between two successive jumps seems to be of the order of 5-10 mm /y. However, it could be reasonable to think that motion rates are higher than average in the period just following a major jump and that they progressively decrease until a new jump takes place. This hypothesis, for instance, could provide an explanation for the relatively high present day velocities indicated by geodetic data with respect to long term motion rates.

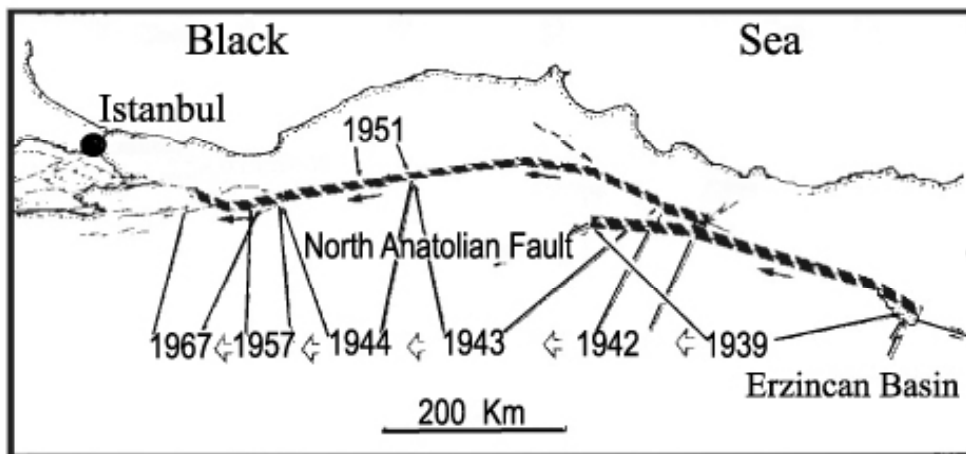


**Fig. 2** - Distribution of surface ruptures of large earthquakes between 1939 and 1967 along the NAF (modified after Barka, 1992).

In order to get insights into the reliability of the above hypothesis, we have tried to quantify the effects, in terms of velocity and stress redistribution over time, of the last acceleration of Anatolia. A first attempt in this sense, based on a simplified model and analytical computations, was carried out by Mantovani et al. (2001a). This work reports the results of a new attempt carried out by adopting a less simplified model.

## 2. Computations of post-seismic relaxation patterns

A 2-D finite element approach has been adopted to compute stress diffusion through an elastic lithosphere coupled with a viscous asthenosphere. The analytical formulation used for computations is described in the Appendix. Fig. 3 shows the geographical contours of the zone considered and the major decoupling zones between the Anatolian-Aegean system and the surrounding area, whose nature and geometry has been chosen on the basis of seismotectonic evidence (Mantovani et al., 2001b). In the model these tectonic belts are simulated by narrow zones where different values of elastic parameters can be adopted with respect to those of the surrounding domain (see Mantovani et al., 2001b, and references therein for details). Segments 1 and 2 correspond to the NAF, segment 3 indicates the westward prolongation of the NAF in the northern Aegean, segment 4 the transcompressional border (Cephalonia line) between the Aegean and Adriatic systems, segment 5 the Hellenic trench, segment 6 the Pliny-Strabo transcompressional trench zone, segment 7 the Cyprus trench zone and segment 8 the east Anatolian fault (e.g., Barka, 1992). Elastic isotropy is assumed in the model (both Lamè constants are  $0.4 \cdot 10^{11}$  Pa, see (A3) in the Appendix). The weak belts simulating collisional

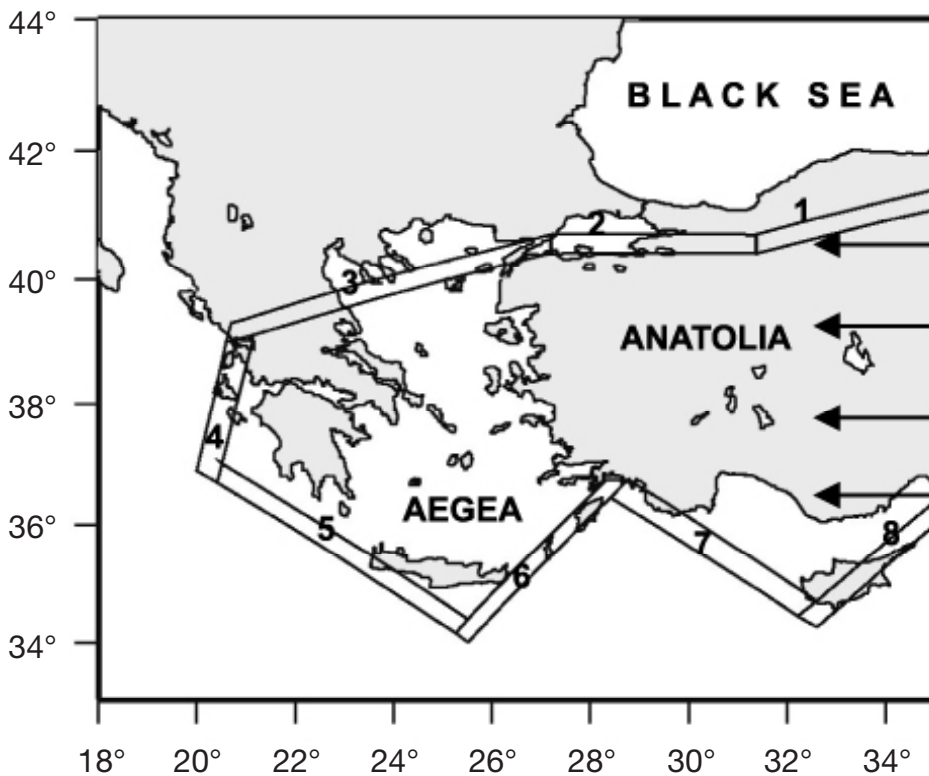


**Fig. 3** - Model adopted in numerical experiments. The decoupling between the Anatolian - Aegean system and the surrounding regions, has been simulated in the model by weak elongated zones (1 to 8). See text for explanations. In these zones, elastic parameters are assumed to be three orders of magnitude lower than those adopted in the remaining model. Black arrows indicate the displacement imposed on the eastern border of the Anatolian wedge. To avoid boundary effects, the northern, western, and southern boundaries of the model are located at  $50^\circ$  N,  $10^\circ$  E, and  $20^\circ$  N respectively. Along these borders displacements normal to the boundary are not allowed.

boundaries or extensional domains (zones 4, 5 and 7) are assumed to be elastically isotropic, with values of the elastic parameters three orders of magnitude lower than those of the surrounding area (see, e.g., Mantovani et al., 2000b, 2001b). Shear zones (1, 2, 3, and 6 in Fig. 3) are assumed to be elastically anisotropic (see, e.g., Lekhnitskii, 1981; Meijer and Wortel, 1996, 1997; Albarello et al., 1997; Mantovani et al., 2000b, 2001b), with values of the shear modulus along the direction of the related structures which are three orders of magnitude lower than that of the surrounding domain.

A crucial choice in our approach concerns the way of stressing the model. In this regard, we think that the sequences of seismic dislocations along the NAF and the other dislocations that occurred before and after the main NAF sequence at the various decoupling zones shown in Fig. 3, could have represented the side effects of a westward acceleration of the whole Anatolian block, triggered by the first strong 1939 shock. In line with this idea, we choose to perturb the model by imposing a unique sudden westward displacement ( $L$ ) at its eastern border (Fig. 3).

In modeling experiments we adopted values of the lithospheric ( $h_l$ ) and asthenospheric ( $h_a$ ) thickness ranging between 50 and 150 km, and of asthenospheric viscosity ( $\eta$ ) ranging between

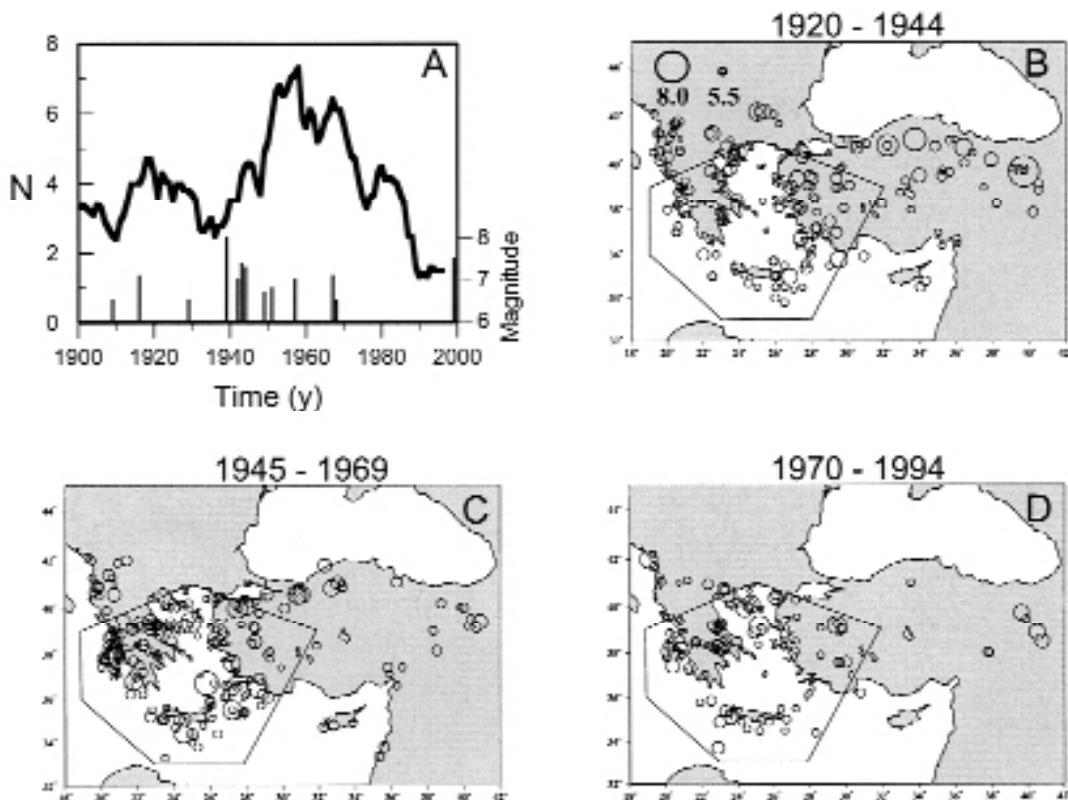


**Fig. 4** - Seismicity pattern (1900-1994) in the western Anatolian-Aegean area. A) Time pattern (thick line) of the number of major earthquakes ( $M > 5.5$ ) in the polygonal area shown in B, C, D.  $N$  is the moving window average (10 years) of the number of events. Before 1900 the seismicity rate is much lower than in the last century, also due to the presumable incompleteness of the earthquake catalogue for  $M > 5.5$  events. Vertical bars at the bottom of the diagram correspond to the major earthquakes (scale on the right) occurred along the NAF. B, C, D) Distribution of major earthquakes ( $M > 5.5$ ) before/during (B) and after (C, D) the main rupture of the NAF (1939 - 1944).

$10^{18}$  and  $10^{19}$  Pa s, as suggested by the reconstruction of rheological profiles in continental zones (e.g. Davaille and Jaupart, 1994; Viti et al., 1997). For the parameter  $L$  we adopted values comprised between 5 and 10 meters. This range is suggested by the seismic slips and fault offsets estimated for the 1939 main shock, which reached maximum values of 7.5 meters (Barka, 1992). The above choice of  $L$  is also based on the conviction that the unique initial displacement imposed on the model should also simulate the effects of all seismic and aseismic movements occurring since 1939 at the various decoupling discontinuities surrounding the Anatolian-Aegean system.

By a trial and error procedure, and by varying the values of the above parameters, we looked for a satisfactory reproduction of the geodetic velocity field (Fig. 1) and of the time pattern of the seismicity rate in the Aegean area (Fig. 4). This last objective was pursued under the tentative hypothesis that seismic activity, in terms of the number of major earthquakes ( $M > 5.5$ ) within a given time interval, is controlled by the amplitude of the average strain energy rate ( $\dot{\Omega} = \Delta\Omega / \Delta t$ ), where  $\Omega$  is expressed by the relation (Ranalli, 1987):

$$\Omega = \frac{1}{2E} [(1 + \nu) (\sigma_{xx}^2 + \sigma_{yy}^2 + 2 \sigma_{xy}^2) - \nu (\sigma_{xx}^2 + \sigma_{yy}^2)] \quad (1)$$

$E$  is the Young modulus,  $\nu$  is the Poisson ratio and  $\sigma_{ij}$  are components of the stress tensor. This choice may find support in the fact that the loading rate controls the effective thickness of the brittle layer (e.g. Ranalli and Murphy, 1987) and thus may have a strong influence on the rate of major events.

Fig. 5 shows the evolution over time of the velocity field for the preferred model parameterization (described in the caption of the figure). It is possible to note that the propagation of the highest velocity values through the elastic layer is retarded by the coupling with the underlying viscous layer. This generates a velocity gradient, with a consequent increase of strain energy rate, whose maximum value gradually migrates through the model. When this “maximum” reaches a tectonic zone it may trigger seismic activity. The migration rate of this phenomenon depends on the model diffusivity  $\beta$  (Rydelek and Sacks, 1990):

$$\beta = \frac{\eta}{Eh_a} \quad (2)$$

Fig. 6 shows how the highest amplitudes of the strain energy rate propagate from east to west through the model. It is interesting to note that this strain pulse reaches the Aegean zone roughly 15-20 years after the beginning of the perturbation, which could account for the observed time pattern of seismic activity (Fig. 4). In order to better illustrate how the predicted pattern can fit the major features of the geodetic kinematic field and of the seismicity distribution over the time, Fig. 7 shows the time patterns of velocity (A), and of the strain energy rate (B) of two points in the model, one in eastern Anatolia and one in the southern Aegean sea. In Fig. 7A it is possible to note that in the time interval 1990-2000, i.e. 50-60 years after the first break of the NAF (1939), the velocity in Anatolia is 17-20 mm /y and in the Aegean is

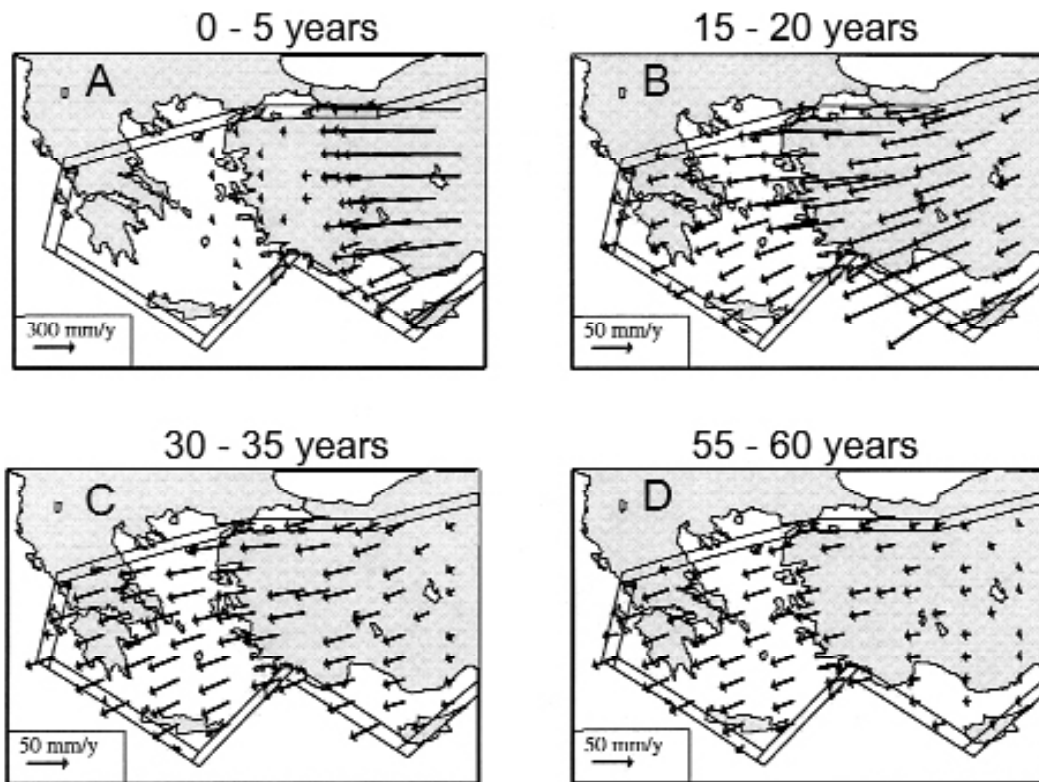


**Fig. 5** - Computed velocity field obtained with the preferred model parameterization: lithospheric thickness ( $h_l$ ) = 110 km, asthenospheric thickness ( $h_a$ ) = 100 km, Young modulus ( $E$ ) =  $10^{11}$  Pa, asthenosphere viscosity ( $\eta$ ) =  $4 \cdot 10^{18}$  Pa s, imposed displacement ( $L$ ) = 7 m. The decoupling zones around the Anatolian - Aegean system (rectangular belts) are of two types: subduction or thrust borders (zones 4, 5, and 7 in Fig. 3), where an  $E$  value of  $10^8$  Pa is adopted, and transcurrent borders (zones 1, 2, 3, 6 and 8) where the shear modulus ( $\mu$ ) in the direction parallel to the related belt is  $10^8$  Pa. Arrows indicate the average rate in the respective time interval.

30-35 mm /y, which agrees fairly well with the geodetic velocities (Fig. 1). The second diagram (Fig. 7B) predicts that the highest values of strain energy rate occur in Anatolia within 10 years and in the Aegean zone roughly 10-30 years after 1939, consistently with the periods of occurrence of the highest seismic activity in the above zones (Fig. 4).

In this attempt, we have not tried to obtain a better fit of the trends of geodetic velocities in the study area (McClusky et al., 2000). For this problem, we make reference to another paper (Mantovani et al., 2001b), where we carried out a more detailed exploration of the effects of lateral heterogeneities and of the geometries and nature of seismotectonic belts in the Anatolian-Aegean system.

In order to get insights into the sensitivity of relaxation processes to the most significant parameters of the model, we carried out some tests, whose results are shown in Fig. 8. The effects of the asthenospheric viscosity are shown in Fig. 8A and 8B. It is interesting to note that relatively small variations of viscosity with respect to the value adopted in the preferred model parameterization, provide an appreciable worsening (roughly 20-30 %) of the match of absolute geodetic velocities in Anatolia and Aegea and of the period of highest seismicity rate in the Aegean area.



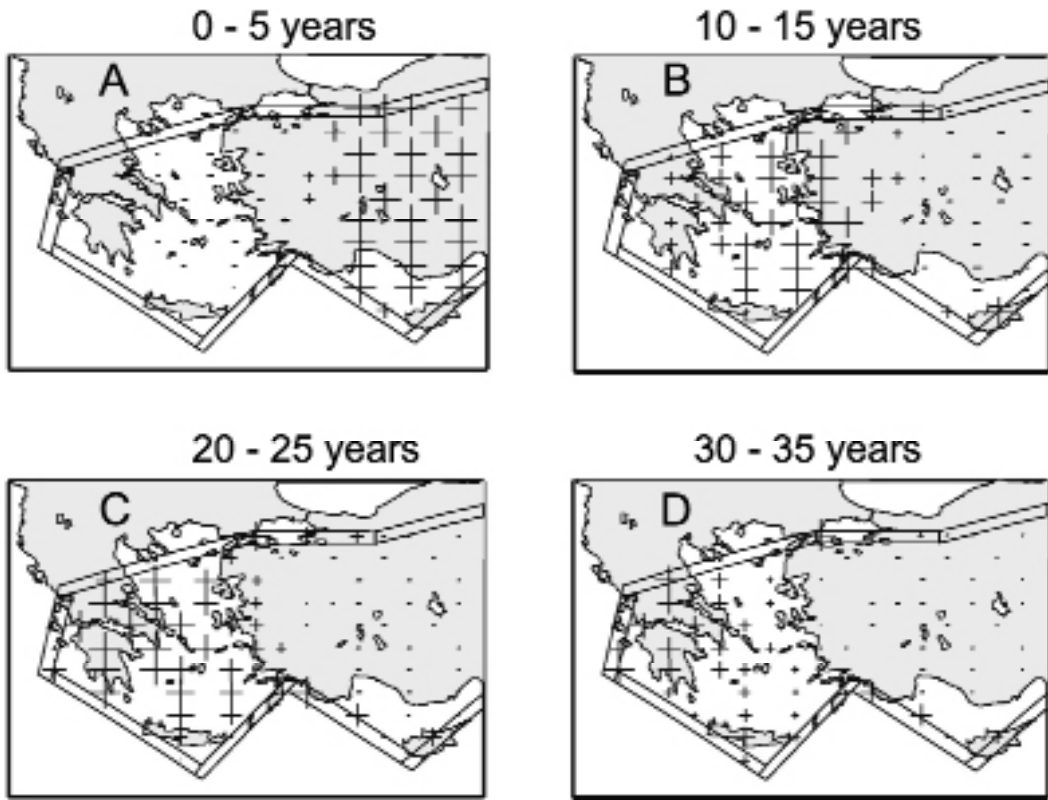


**Fig. 6** - Patterns of normalized strain energy rates for the preferred model parameterization (see the caption of Fig. 5) in the time intervals reported over the pictures. Crosses and bars respectively indicate increases and decreases of strain energy rate in the respective time intervals.

Figs. 8C and 8D illustrate the effect of varying lithospheric thicknesses. The results obtained show that in the period considered (50-60 years) the velocities in the Aegean and Anatolian zones are not very sensitive to this parameter. An appreciable effect is obtained only

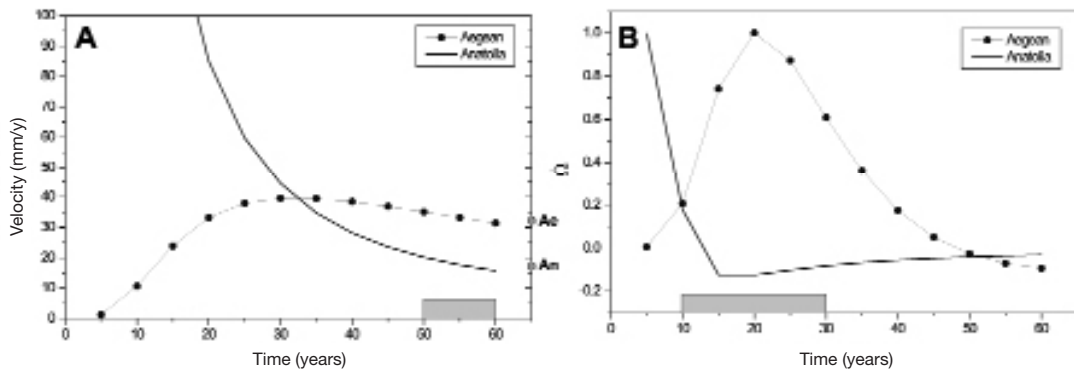


**Fig. 7** - Time patterns of velocity (A) and normalized strain energy rate (B) at two points, one in Aegea (37°N, 25°E) and the other in Anatolia (39°N, 32°E). The gray band along the time axis in A identifies the time interval covered by geodetic observations (1990-2000). The gray band along the time axis in B identifies the time interval where the highest seismicity rates occur in the Aegean area (see Fig. 4A). The symbols Ae and An on the right velocity axis indicate the values of geodetic velocities observed in the Aegea and Eastern Anatolia (Fig. 1).

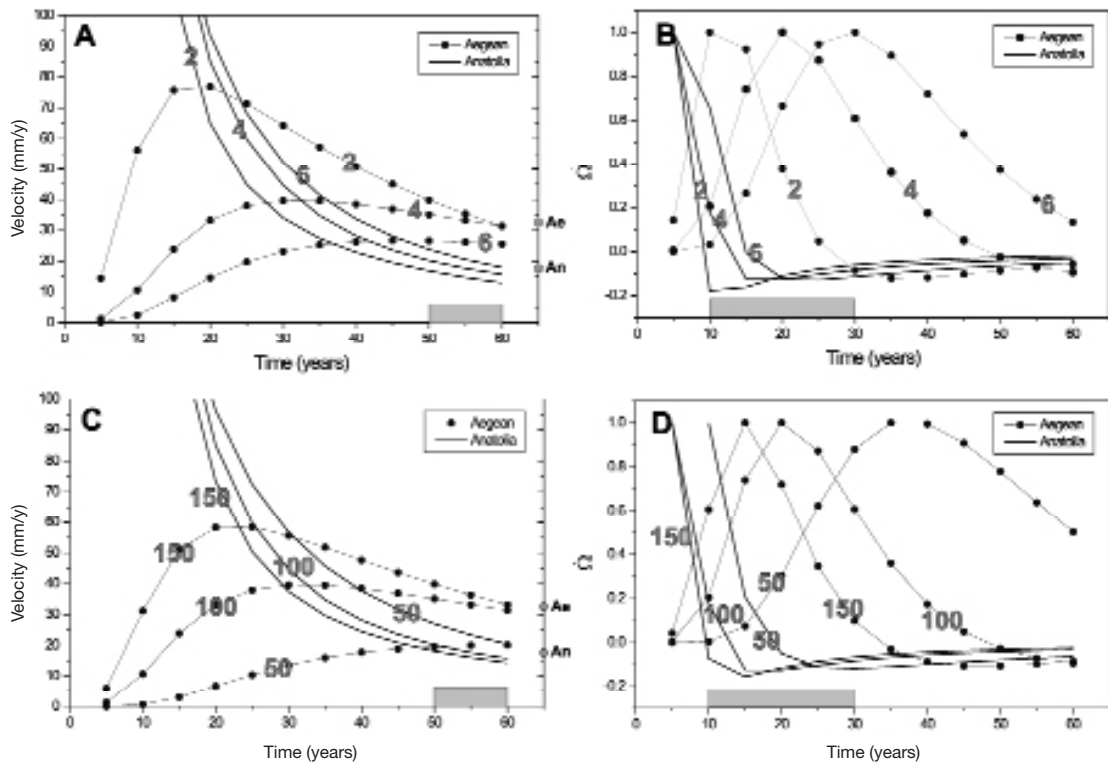


**Fig. 8** - Sensitivity of the time patterns of velocity and normalized strain energy rate to some model parameters. A, B) Time patterns of velocity and normalized strain energy rate computed for different values of viscosity ( $\eta$ ) at the two points in Aegea and Anatolia mentioned in the caption of Fig. 7. Numbers on curves refer to values of  $\eta$  (in units of  $10^{18}$  Pa s). C, D) Variation of lithospheric thickness (km). See caption of Fig. 7 for the meaning of the other symbols. Comments in the text.

by assuming a relatively low value of thickness (50 km). Analogous observations could be made for the time pattern of strain energy rate (Fig. 8D). It must be pointed out that the results shown in Fig. 8C and 8D may be related either to  $h_l$  or  $h_a$ , since these two parameters have the same influence on the model diffusivity. For the same reason, there is an intrinsic ambiguity about the effects of all single parameters controlling the model diffusivity Eq. 2. Thus, the match of observable, i.e. the geodetic velocities and the time pattern of seismicity rate, in the Anatolian-Aegean area can only provide information on the combination of the above parameters.

### 3. Conclusions and discussion

The present day kinematic pattern in the Anatolian-Aegean system, inferred from space geodetic data is significantly different from the long term pattern suggested by offset measurements along the NAF and by the seismic history of this major fault system. Quantification of post seismic relaxation processes in the study area indicates that the geodetic kinematic pattern could be explained as a consequence of the last major acceleration of Anatolia, triggered by the last seismic sequence along the NAF. This result suggests that the

westward drift of Anatolia could be not continuous over time. Sudden accelerations may occur after major seismic sequences along the NAF and then velocities progressively decrease up to the next acceleration. Seismicity information suggests that major jumps have recurrence time intervals of several hundreds of years. In particular, the previous NAF's activation occurred roughly 900 years before the last one.

The coupling of the lithosphere with the underlying lithosphere produces a slow migration of displacements and stresses induced by sudden accelerations in eastern Anatolia, which results in a progressive westward propagation of the zones where the highest velocities and strain energy rate occur. This phenomenon can account for the fact that present day velocities (GPS) in the Aegean area are higher than those observed in Anatolia also for the fact that the maximum release of seismic energy in the Aegean zone has occurred some tens of years after the first large break of the NAF. In particular, the results obtained in this work indicate that under realistic structural and rheological conditions ( $h_l = 110$  km,  $h_a = 100$  km, and  $\eta = 4 \cdot 10^{18}$  Pa s) it is possible to obtain a fairly good match of the absolute velocities in Anatolia (18-24 mm /y) and Aegea (32 mm /y) and of the periods during which the highest seismicity rate occurs in the Anatolian and Aegean zones.

The sensitivity of the relaxation patterns to the asthenospheric viscosity and to lithospheric and asthenospheric thickness has been explored.

The results obtained in this work might have implications on the understanding of the geodynamic setting in the study area. In particular, they demonstrate that the higher present day velocities in the Aegean region with respect to Anatolia must not necessarily be interpreted as an effect of a slab pull mechanism in the Hellenic Arc. In this regard, one should also consider that another important aspect of the geodetic velocity field, i.e. the almost uniform distribution of velocities within the Aegean area (Fig. 1), is significantly different from the kinematic pattern one would expect from the presumed slab pull mechanism. Such model, in fact, would require a divergence between the Hellenic Arc and the internal area (central-northern Aegean), able to produce extension in the back arc zone, i.e. the Cretan basin. More in general, the uniform velocity field suggested by geodetic data in the Aegean zone can hardly be reconciled with the observed long term deformation pattern in this zone, which implies an heterogeneous kinematic behavior.

The evidence and arguments mentioned above support the hypothesis that the present day kinematics of the study area can most likely represent a transient effect, connected with the post-seismic relaxation described earlier.

Other doubts about the reliability of the slab-pull model are suggested by the analysis of the recent/present strain pattern in the Aegean zone and surroundings, deduced from geological and geophysical observations. This evidence points out that in the last My extensional deformation has mainly occurred in the eastern Cretan basin, with a roughly NW-SE trend, and in the north Aegean trough, with a roughly N-S trend, associated to a dominant dextral shear (e.g. Angelier et al., 1982; Mercier et al., 1987; Hatzfeld et al., 1999). Such pattern can not easily be interpreted as an effect of the gravitational sinking of the Hellenic slab, and of the consequent trench suction force roughly oriented SW-NE.

Another major problem of the slab pull model is explaining why extensional tectonics, with

a NE-SW trend, ceased around the late Pliocene/early Quaternary in the western Cretan basin, in spite of the fact that this kind of deformation would be strongly favored by the southwestward trench suction force induced by presumed roll back of the Ionian-Levantine slab.

Other evidence and arguments which could help to discriminate between the two geodynamic models mentioned above may be provided by the analysis of the space-time distribution of major Plio-Quaternary tectonic events (Mantovani et al., 1997, 2000a, 2000b) and by numerical modeling experiments in the eastern Mediterranean area (Mantovani et al., 2000c, 2001b).

## References

- Albarelo D., Mantovani E. and Viti M.; 1997: *Finite element modeling of the recent/present deformation pattern in the Calabrian Arc and surrounding regions*. *Annali di Geofisica* **40**, 833-848.
- Ambraseys N. N.; 1988: *Engineering seismology*. *Earthquake Engineering and Structural Dynamics*, **17**, 1-103.
- Anderson D. L.; 1975: *Accelerated plate tectonics*. *Science*, **167**, 1077-1079.
- Angelier J., Lyberis N., Le Pichon X., Barrier E. and Huchon P.; 1982: *The tectonic development of the Hellenic arc and the sea of Crete: a synthesis*. *Tectonophysics*, **86**, 139-196.
- Barka A. A.; 1992: *The North Anatolian fault zone*. *Annales Tectonicae*, **6**, 164-195.
- Davaille A. and Jaupart C.; 1994: *Onset of thermal convection in fluids with temperature dependent viscosity: application to oceanic mantle*. *J. Geophys. Res.*, **99**, 19853-19866.
- Elsasser W. M.; 1969: *Convection and stress propagation in the upper mantle*. In: Runcorn S.K. (ed), *The application of Modern Physics to the Earth and Planetary Interiors*, Wiley, New York, pp. 223-246.
- Hatzfeld D., Ziazia M., Kementzetzidou D., Hatzidimitriou P., Panagiotopoulos D., Makropoulos K., Papadimitriou P. and Deschamps A.; 1999: *Microseismicity and focal mechanisms at the western termination of the North Anatolian Fault and their implications for continental tectonics*. *Geophys. J. Int.*, **137**, 891-908.
- Ikeda Y.; 1988: *Recent activity of the Iznik-Mekece fault at Corak Stream, east of Iznik*. In: Honkura Y. and Isikara A.M. (eds), *Multidisciplinary research on fault activity in the western part of the North Anatolian Fault Zone*, pp. 15-27.
- Ikeda Y., Suzuki Y., Herece E., Saroglu F., Isikara A. M., and Honkura Y.; 1991: *Geological evidence for the last two faulting events on the North Anatolian fault zone in the Mudurnu Valley, western Turkey*. *Tectonophysics*, **193**, 335-345.
- Jackson J. and McKenzie D.; 1984: *Active tectonics of the Alpine-Himalayan belt between western Turkey and Pakistan*. *Geophys. J.R. Astr. Soc.*, **77**, 185-264.
- Jackson J. and McKenzie D.; 1988: *The relationship between plate motions and seismic moment tensors, and the rates of active deformation in the Mediterranean and Middle East*. *Geophys. J.*, **93**, 45-73.
- Kostrov V. V.; 1974: *Seismic moment and energy of earthquakes, and seismic flow of rocks*. *Izv. Earth. Phys.* **1**, 23-40.
- Lekhnitskii S. G.; 1981: *Theory of elasticity of an anisotropic body*. Mir publ., Moscow, 430 pp.
- Le Pichon X., Chamot-Rooke N., Lallemand S., Noomen R. and Veis G.; 1995: *Geodetic determination of the kinematics of central Greece with respect to Europe: implications for Eastern Mediterranean tectonics*. *J. Geophys. Res.*, **100**, 12675-12690.
- Mantovani E., Albarello D., Tamburelli C., Babbucci D. and Viti M.; 1997: *Plate convergence, crustal delamination, extrusion tectonics and minimization of shortening work as main controlling factors of the recent Mediterranean deformation pattern*. *Annali di Geofisica*, **40**, 611-643.

- Mantovani E., Albarello D., Babbucci D., Tamburelli C. and Viti M.; 2000a: *Genetic mechanism of back-arc opening: insights from the Mediterranean deformation pattern*. In: Boschi E., Ekstrom G. and Morelli A. (eds), *Problems in Geophysics for the New Millennium*, Editrice Compositori, Bologna, pp. 151-178.
- Mantovani E., Viti M., Albarello D., Babbucci D., Tamburelli C. and Cenni C.; 2000b: *Generation of back arc basins in the Mediterranean region: driving mechanism and quantitative modelling*. *Boll. Soc. Geol. It.*, in press.
- Mantovani E., Viti M., Albarello D., Tamburelli C., Babbucci D. and Cenni N.; 2000c: *Role of kinematically induced horizontal forces in Mediterranean tectonics: insights from numerical modelling*. *J. Geodynamics*, **30**, 287-320.
- Mantovani E., Viti M., Cenni N., Albarello D. and Babbucci D.; 2001a: *Short and long term deformation patterns in the Aegean-Anatolian systems: insights from space geodetic data (GPS)*. *Geophys. Res. Lett.*, **28**, 2325-2328.
- Mantovani E., Cenni N., Albarello D., Viti M., Babbucci D., Tamburelli C. and D'Onza F.; 2001b: *Numerical simulation of the observed strain field in the central-eastern Mediterranean region*. *J. Geodynamics*, **31**, 519-556.
- McClusky S., Balassanian S., Barka A., Demir C., Ergintav S., Georgiev I., Gurkan O., Hamburger M., Hurst K., Khale H., Kastens K., Kekelidze G., King R., Kotzev V., Lenk O., Mahmoud S., Mishin A., Nadariya M., Ouzounis A., Paradissis D., Peter Y., Prilepin M., Reilinger R., Sanli I., Seeger H., Tealeb A., Toksoz M. N. and Veis G.; 2000: *Global positioning system constraints on plate kinematics and dynamics in the eastern Mediterranean and Caucasus*. *J. Geophys. Res.*, **105**, 5695-5719.
- Meijer P. Th. and Wortel M. J. R.; 1996: *Temporal variation in the stress field of the Aegean region*. *Geophys. Res. Letters*, **23**, 439-442.
- Meijer P. Th. and Wortel M. J. R.; 1997: *Present-day dynamics of the Aegean region: a model analysis of the horizontal pattern of stress and deformation*. *Tectonics*, **16**, 879-895.
- Mercier J., Sorel D. and Simeakis K.; 1987: *Changes in the state of stress in the overriding plate of a subduction zone: the Aegean Arc from the Pliocene to the Present*. *Ann. Tectonicae*, **1**, 20-39.
- Mercier J. L., Simeakis K., Sorel D. and Vergely P.; 1989: *Extensional tectonic regimes in the Aegean basins during the Cenozoic*. *Basin Research*, **2**, 49-71.
- Pollitz F., Burgmann R. and Romanowicz B.; 1998: *Viscosity of oceanic lithosphere inferred from remote triggering of earthquakes*. *Science*, **280**, 1245-1249.
- Pondrelli S., Morelli A. and Boschi E.; 1995: *Seismic deformation in the Mediterranean area estimated by moment tensor summation*. *Geophys. J. Int.*, **122**, 938-952.
- Press W., Flannery B., Tenkolsky S. and Vetterling W.; 1992: *Numerical recipes*. 2nd edn. Cambridge University Press. Cambridge, 818 pp.
- Ranalli G.; 1987: *Rheology of the earth*. Allen and Unwin, Winchester, USA, 366 pp.
- Ranalli G. and Murphy D.G.; 1987: *Rheological stratification of the lithosphere*. *Tectonophysics*, **132**, 281-295.
- Rydelek P. A. and Sacks I. S.; 1990: *Asthenospheric viscosity and stress diffusion: a mechanism to explain correlated earthquakes and surface deformation in NE Japan*. *Geophys. J. Int.*, **100**, 39-58.
- Sewell G.; 1981: *A small general purpose Finite Element program*. IMSL technical report n. 8102.
- Sewell G.; 1985: *Analysis of a Finite Element Method PDE/PROTRAN*. Springer Verlag, Berlin, 154 pp.
- Tapponnier P.; 1977: *Evolution tectonique du système alpin en Méditerranée: poinçonnement et écrasement rigide-plastique*. *Bull. Soc. Géol. Fr.*, **19**, 437-460.
- Taymaz T., Jackson J. and McKenzie D.; 1991: *Active tectonics of the North and Central Aegean Sea*. *Geophys. J. Int.*, **106**, 433-490.
- Viti M., Albarello D. and Mantovani M.; 1997: *Rheological profiles in the central-eastern Mediterranean*. *Annali di Geofisica*, **40**, 849-864.
- Viti M., Albarello D. and Mantovani E.; 2001: *Classification of seismic strain estimates in the Mediterranean region from a "bootstrap" approach*. *Geophys. J. Int.*, **146**, 399-415.

## Appendix

The model is composed of an elastic lithosphere mechanically coupled to an underlying viscous asthenosphere. In the Elsasser's (1969) approximation, the viscous stresses at the basis of the lithosphere are:

$$\begin{aligned}\sigma_{xz}^* &\equiv \frac{\eta}{h_a} \frac{\partial u_x}{\partial t} \\ \sigma_{yz}^* &\equiv \frac{\eta}{h_a} \frac{\partial u_y}{\partial t}\end{aligned}\tag{A1}$$

where  $u_i$  is the displacement,  $t$  is time,  $\eta$  is the Newtonian viscosity and  $h_a$  is the thickness of asthenosphere. The  $z$  axis is vertical. In the thin sheet approximation, the dynamic equilibrium in the lithosphere requires that:

$$\begin{aligned}\frac{\partial}{\partial x} (h_l \sigma_{xx}) + \frac{\partial}{\partial y} (h_l \sigma_{xy}) &= \sigma_{xz}^* \\ \frac{\partial}{\partial x} (h_l \sigma_{yx}) + \frac{\partial}{\partial y} (h_l \sigma_{yy}) &= \sigma_{yz}^*\end{aligned}\tag{A2}$$

where  $\sigma_{ij}$  represent the components of the lithospheric stress tensor averaged over a thickness  $h_l$ .

By assuming that lithosphere behaves as an elastic body, (A2) can be expressed in terms of displacement components  $u_x$  and  $u_y$  in the form:

$$\begin{aligned}\frac{\partial}{\partial x} \left\{ C_1 \frac{\partial u_x}{\partial x} + C_2 \frac{\partial u_y}{\partial y} \right\} + \frac{\partial}{\partial y} \left\{ C_3 \left[ \frac{\partial u_x}{\partial y} + \frac{\partial u_y}{\partial x} \right] \right\} &= \frac{\eta}{h_a} \frac{\partial u_x}{\partial t} \\ \frac{\partial}{\partial x} \left\{ C_4 \left[ \frac{\partial u_x}{\partial y} + \frac{\partial u_y}{\partial x} \right] \right\} + \frac{\partial}{\partial y} \left\{ C_5 \frac{\partial u_y}{\partial y} + C_6 \frac{\partial u_x}{\partial x} \right\} &= \frac{\eta}{h_a} \frac{\partial u_y}{\partial t}\end{aligned}\tag{A3}$$

where  $C_i$  ( $i = 1,6$ ) represent the elastic constants of the lithosphere and are a function of the position.

In the case of elastic isotropy, coefficients  $C_i$  are given by

$$\begin{aligned}C_1 = C_6 &= h_l (\lambda + 2\mu) \\ C_2 = C_5 &= h_l \lambda \\ C_3 = C_4 &= h_l \mu\end{aligned}$$

where  $\lambda$  and  $\mu$  are the Lamè's constants.

In the case of elastic anisotropy, coefficients  $C_i$  will also depend on the direction of anisotropy (see e.g., Lekhnitskii, 1981).

The (A3) is solved numerically. The implicit Crank-Nicolson method (see, e.g., Press et al., 1992) is used to discretize time and to reduce parabolic form of (A3) to a non-homogeneous elliptic form which is solved by a Finite Element approach (see for details Sewell, 1981, 1985).